Noble-metal–CdTe interface formation

D. J. Friedman, I. Lindau, and W. E. Spicer
Stanford Electronics Laboratories, Stanford University, Stanford, California 94305
(Received 11 June 1987)

The room-temperature Au/*p*-type CdTe, Ag/*n*-type CdTe, Cu/*n*-type CdTe, and Cu/*p*-type CdTe interfaces have been studied with x-ray and ultraviolet photoelectron spectroscopy for the cleaved CdTe(110) surface. These interfaces are all found to be nonabrupt, with a significant concentration of dissociated Te in the overlayer for all three overlayer metals. The corresponding noble-metal interfaces with $Hg_{1-x}Cd_xTe$ are discussed with respect to these results. The final position of the surface Fermi level E_F for each interface is $E_F - E_{VBM} = 0.95 \pm 0.1$ eV for Ag/*n*-type CdTe, 1.0 ± 0.1 eV for Cu/*n*-type CdTe, 0.9 ± 0.1 eV for Cu/*p*-type CdTe, and 0.8 ± 0.1 eV for Au/*p*-type CdTe. From these results one would expect Schottky barriers between 0.5 and 0.7 eV for these metals on *n*-type CdTe.

I. INTRODUCTION

In the study of metal-semiconductor interfaces, the morphology of the interface is of interest both intrinsically, since the driving forces behind the observed interfacial chemistry are still not fully understood, and also because of the interplay between interface morphology and Schottky-barrier height. Studying the interfaces with II-VI compound semiconductors such as CdTe is also of relevance to III-V compound semiconductor interface research, as the greater ionicity of the II-VI compound semiconductor provides insight into the role of cation–anion bonding in interface formation.[1] This paper presents a photoemission study of noble-metal interfaces with CdTe: more specifically, the Au/*p*-type CdTe, Ag/*n*-type CdTe, Cu/*n*-type CdTe, and Cu/*p*-type CdTe interfaces. Bulk thermodynamic data relevant to the determination of the interface morphology are given in Table I, which shows heats of metal-telluride formation from Ref. 2 as well as calculated heats of alloying $\Delta H_{sol}(Cd;M)$ of Cd at infinite dilution in the overlayer metals (M).

CdTe is not only of practical interest, for instance for solar-cell technology, but also serves as a prototypical II-VI semiconductor for the purposes of interface research. Previous studies[3–5] of metal interfaces with the cleaved CdTe(110) surface have tended to concentrate more on the Schottky-barrier height than on the interface morphology, while both will be emphasized in this paper. Finally, studying the metal/CdTe interface is helpful in understanding the more complex metal-$Hg_{1-x}Cd_xTe$ interface, in which there has recently been increasing interest.[6–12] $Hg_{1-x}Cd_xTe$ (MCT), a pseudobinary alloy with a band gap[13] varying from 0 to 1.50 eV (at 300 K) as the composition is varied from $x=0$ to 1, is of technological importance as an infrared detector. Related to the variable band gap is a marked instability in the Hg—Te bond,[14] which in turn plays a crucial role in metal-MCT interface properties. A comparison with the corresponding metal-CdTe interfaces will thus assist in the understanding of the role of the Hg bond in metal-MCT interface formation.

II. EXPERIMENT

Single-crystal bars of CdTe (*p*-type for the Au/CdTe study and *n*-type for the Ag/CdTe and Cu/CdTe studies) with cross-sectional areas of $\sim 5 \times 5$ mm^2 were transferred into a previously baked vacuum chamber and then cleaved in ultrahigh vacuum (base pressure less than 1×10^{-10} Torr) to reveal a (110) face. Sequential depositions of metal were performed on the room-temperature surface from a tungsten filament, with overlayer thicknesses monitored with a quartz-crystal microbalance. The amount of metal deposited is given in units of Å and monolayers (ML), which we define to be the surface density of atoms on the CdTe(110) face: 1 ML equals 6.76×10^{14} atoms/cm^2, which corresponds to 1.15 Å of metallic Au, 1.15 Å of metallic Ag, and 0.80 Å of metallic Cu. ML is the more appropriate unit for low coverages. The surface was studied at each coverage by x-ray and ultraviolet photoelectron spectroscopy (XPS and UPS) using, respectively, a Mg $K\alpha$ x-ray source ($h\nu = 1253.6$ eV) and a helium lamp (He I and He II, $h\nu = 21.2$ and 40.8 eV); the photoelectrons were analyzed with a double-pass cylindrical mirror analyzer (CMA).

III. RESULTS: Au/*p*-TYPE CdTe

A. Overlayer adsorption

Figures 1(a) and 2 show He I spectra of the valence band and the Cd 4*d* shallow core level as a function of Au deposition. From the spectral region near the Fermi level E_F, shown in the inset of Fig. 1, it can be seen that by $\Theta = 0.5$ ML there is clear emission to E_F; a metallic Fermi edge can be detected by $\Theta = 2$–4 ML. The occurrence (implied by the presence of the Fermi edge) of some fraction of the overlayer in the metallic state at a coverage as low as 2 ML suggests that at this coverage

 ©1988 The American Physical Society

the deposited Au has formed clusters (possibly containing Cd or Te atoms dissociated from the semiconductor surface) large enough to support a Fermi surface.

By 1-ML coverage, emission from the Au $5d$ states is visible in the spectra; as more metal is deposited, the Au $5d$ spectrum undergoes an ~ 0.2-eV shift to higher kinetic energy. A similar shift (~ 0.4 eV to higher kinetic energy, mostly completed by $\Theta = 10$ ML) also occurs in the Au $4f$ states. The higher Au $4f$ binding energy at the lowest coverages is consistent with either Au adsorption as a reacted Au-Te phase or with the cluster formation mentioned above, as clusters would have a higher binding energy than the pure metal.[15]

The valence-band spectrum undergoes a continuous evolution in shape, approaching a stable line shape by about $\Theta = 10$ ML. This line shape, while dominated by emission from Au-derived states, does not quite correspond to the line shape of elemental Au, as can be seen from Fig. 1(b) which compares the valence-band spectrum of 20 Å (17 ML) Au/CdTe with an Au–stainless-steel reference spectrum. Since the He I spectrum probes only the top 10–20 Å of the surface, we take the departure of the 20-Å Au/CdTe valence band from that of pure Au to indicate the presence of Cd and/or Te dissociated from the semiconductor and intermixed into the overlayer.

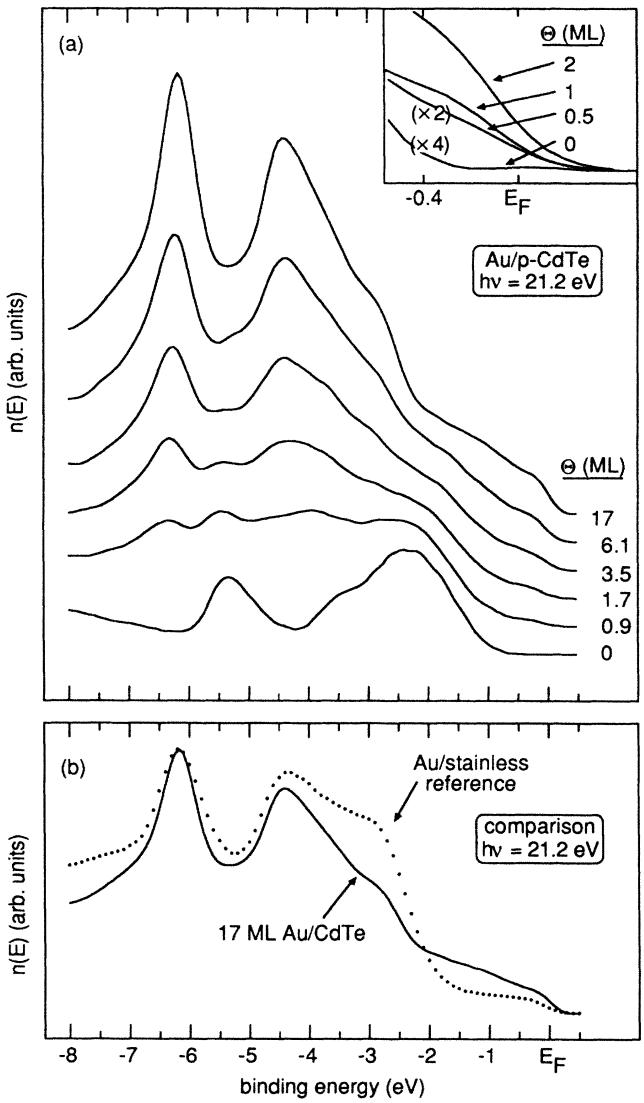

FIG. 1. (a) He I ($h\nu = 21.2$ eV) spectra of the valence band with increasing coverage of Au on CdTe. (b) Comparison of the He I valence-band spectrum of 17 ML Au/CdTe with an Au–stainless-steel reference spectrum.

B. Te dissociation

The presence of significant quantities of a semiconductor component in the overlayer would result in a greater photoemission intensity from that component than would be observed for an abrupt laminar overlayer. Figure 3(a) plots the attenuation with overlayer coverage of the Cd and Te core-level intensities I, normalized to their zero-coverage values I_0. Below about 30-Å coverage, the Te $3d$ signal attenuates roughly in exponential form with a rate corresponding to an escape length of about 20–25 Å, consistent with a reasonably abrupt interface. However, above about 30-Å coverage the Te intensity starts to level off, so that even at 200 Å it is still about 15% of its initial intensity. This lack of attenuation is too pronounced to be attributable entirely to islanding (although some degree of islanding cannot be explicitly ruled out), and thus provides an unambiguous signature of the presence of Te in the overlayer.

The Te $3d$ and $4d$ core levels excited by Mg $K\alpha$ light

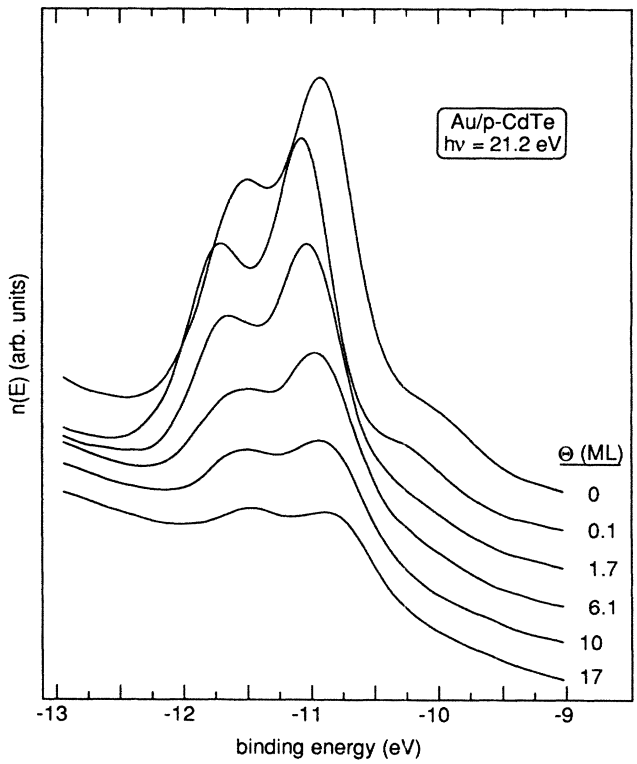

FIG. 2. He I ($h\nu = 21.2$ eV) spectra of the Cd $4d$ shallow core levels with increasing coverage of Au on CdTe. Energies are referred to E_F.

appear, respectively, at 670 and 1200 eV kinetic energy, so that the Te 4*d* probe is more bulk sensitive. Defining the escape lengths for Te 3*d* and Te 4*d* photoelectrons as λ_{3d} and λ_{4d}, respectively, then $\lambda_{4d} > \lambda_{3d}$ due to the higher kinetic energy of the Te 4*d* photoelectrons.[16] Thus, comparison of the attenuation with overlayer deposition of the Te 3*d* and 4*d* core intensities can provide information on the distribution of Te in the overlayer. Figure 3(b) shows the intensity ratio $R(\Theta) \equiv I_{\mathrm{Te}\,3d}(\Theta)/I_{\mathrm{Te}\,4d}(\Theta)$ normalized to the zero-coverage value $R(0)$. If the dissociated Te were distributed uniformly throughout the overlayer (at a density less than in bulk CdTe), $R(\Theta)$ would decrease with increasing overlayer coverage. However, Fig. 3(b) shows that at $\Theta \approx 30$ Å, $R(\Theta)/R(0)$ starts to rise, reaching a value of about 1.3 by 100-Å coverage. This increase in the more surface-sensitive Te 3*d* signal relative to the Te 4*d* indicates that most of the dissociated Te is within roughly the Te 3*d* escape length λ_{3d} of the surface, so that the Te 3*d* signal is more dominated by the dissociated Te than is the less surface-sensitive Te 4*d* signal. Thus, the difference in Te 3*d* and Te 4*d* attenuation rates indicates the development of a Te-rich layer segregated at or near the surface of the overlayer, as opposed to a uniform distribution of Te in the overlayer. A comparison of Figs. 3(a) and 3(b) shows that $R(\Theta)/R(0)$ starts to rise at the same coverage (~ 30 Å) at which the Te attenuation rate starts to slow from its original "abruptlike" rate. Thus, the onset of large-scale Te dissociation occurs at about 30-Å coverage, and as the Te is pulled from the surface of the semiconductor above this coverage it is segregated towards the surface of the overlayer.

It was shown in Sec. III A that the Au within a photoelectron escape length (20–30 Å) of the surface of the overlayer is not in pure elemental form even at high coverages. The much faster attenuation and consequent lower signal intensity at high coverages of the Cd 3*d* compared to the Te 3*d*, as seen in Fig. 3(a), implies that the Cd concentration in the near-surface region of the overlayer is negligible compared to the Te concentration. The evolution of the Te 3*d* and Au 4*f* core-level widths with coverage, reflecting the chemical interaction of these two elements as the interface is formed, is shown in Fig. 4. As metal is deposited upon the semiconductor, the Te signal, which at zero coverages arises solely from Te in the CdTe lattice, acquires contributions from Te bound to Au, probably with several kinds of inequivalent lattice sites, and the width of the total XPS Te 3*d* signal increases. Conversely, the width of the Au signal drops with increasing coverage, as the distribution of the number of Te atoms seen by a given Au atom becomes more uniform with increasing coverage. Furthermore, cluster-size effects, which play an important role in the overlayer metal's core-level binding energy at low coverages and small cluster sizes, become less important with increasing coverage and larger cluster sizes.

C. Cd dissociation and band bending

As reflected in the Cd 4*d* core levels in Fig. 2, between zero coverage and $\Theta = 0.1$ ML there is a rigid shift of the energy bands 0.15 ± 0.05 eV to higher binding energy. Using the value of $E(\mathrm{Cd}\ 4d_{5/2}) - E_{\mathrm{VBM}} = -10.3$ eV in CdTe,[17] the result of this initial band bending is to put the Fermi level 0.8 ± 0.1 eV above the valence-band maximum (VBM) at $\Theta = 0.1$ ML. However, the band-bending behavior at higher coverages is not immediately clear: the band bending may be deduced only from the

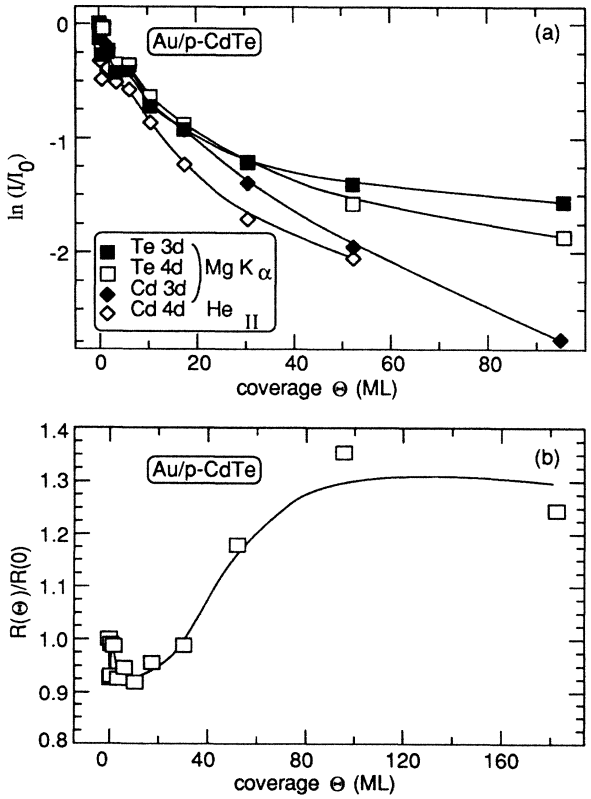

FIG. 3. (a) Attenuation (natural log scale) of the XPS peak areas I of the CdTe core levels with increasing Au coverage. The peak areas are normalized to their zero-coverage values I_0. (b) The intensity ratio $R(\Theta) \equiv I_{\mathrm{Te}\,3d}(\Theta)/I_{\mathrm{Te}\,4d}(\Theta)$ normalized to the zero-coverage value $R(0)$, for Au/CdTe.

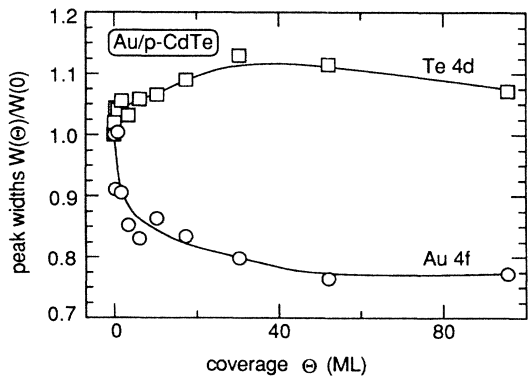

FIG. 4. Variation of the Te 3*d* and Au 4*f* core widths (FWHM) with coverage for Au/CdTe. The widths are normalized to the 0-ML coverage for the Te 3*d* core level, and to the 0.1-ML coverage for the Au 4*f* core level.

substrate photoelectron signal, which must therefore be deconvolved from contributions which may arise from dissociated Cd or Te atoms intermixed into the overlayer. Thus, while Fig. 2 appears to show a gradual shift of the Cd 4*d* core level to higher kinetic energy which might at first glance be interpreted as being due to further band bending, the possibility must be considered that what is instead being observed is an increasingly intense contribution, at higher kinetic energy than the substrate peak, from dissociated Cd. Thus the question of Cd dissociation is important not only for understanding the morphology of the interface, but also for determining the band bending and consequently the Schottky-barrier height due to the interface.

The attenuation of the Cd 4*d* intensity at $h\nu=40.8$ eV, shown in Fig. 3(a), is much too slow to be consistent with an abrupt laminar interface, since at $h\nu=40.8$ eV the Cd 4*d* core level appears at a kinetic energy of about 25 eV with a corresponding photoelectron escape length on the order of 5 Å. Taken by itself, the Cd 4*d* attenuation rate is thus consistent with Cd dissociation or with cluster formation of the overlayer, which would also result in a reduced attenuation rate of the Cd signal intensity. Less ambiguous evidence for the influence of dissociated Cd in the Cd 4*d* signal is provided by a comparison of the Cd 4*d* (He II light) and Cd 3*d* (Mg $K\alpha$ light, kinetic energy of $\sim$840 eV) centroids, shown in Fig. 5. The variation of photoelectron escape length with kinetic energy is discussed in Ref. 16. Because the Cd 3*d* signal is much more bulk sensitive (photoelectron escape length of $\sim$20 Å) than the Cd 4*d* signal (escape length of $\sim$5 Å), at coverages below about 10 Å the Cd 3*d* signal will be dominated by the substrate contribution, and thus will be a much better indicator of the substrate's band bending than the Cd 4*d* signal would be. The leveling off of the Cd 3*d* peak position from low coverages all the way up to the highest coverage (10–20 Å) for which the Cd 3*d* signal is still dominated by the substrate, indicates that the band bending is indeed complete at monolayer coverages, and that the drift of the Cd 4*d* signal to lower binding energy is in fact due to increasing contribution from dissociated Cd. It should be noted that Patterson and Williams[5] reported no Cd dissociation in their studies of the Au/*n*-type CdTe interface, although their photoelectron spectra are in fact consistent with ours.

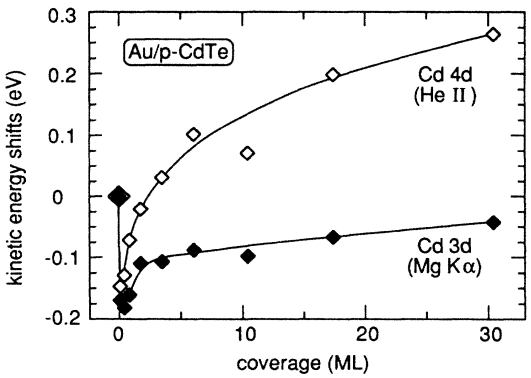

FIG. 5. Comparison of the kinetic-energy shifts of the Cd 4*d* ($h\nu=40.8$ eV) and Cd 3*d* ($h\nu=1253.6$ eV) centroids as a function of Au coverage. The shifts are defined to be zero at $\Theta=0$ ML for both the 4*d* and 3*d* core levels, as indicated by the superposed solid diamond (Cd 3*d*) and open diamond (Cd 4*d*) symbols at $\Theta=0$ ML. Note the shift of $\sim$0.15 eV to lower kinetic energy between $\Theta=0$ and 0.1 ML for both core levels.

The binding energy of the dissociated cation core level can give information concerning the chemical environment seen by the dissociated species.[18] In the present case there are essentially three possibilities: the dissociated Cd may be segregated in pure metallic form, it may be alloyed with the Au overlayer, or there may be some dissociated Te in its local environment as well. Pure metallic Cd has a $4d_{5/2}$ binding energy of -10.6 eV,[19] while the binding energy for Cd alloyed in Au will be shifted from this pure metal value by an amount which can be calculated[18,20] from a Born-Haber cycle argument using as inputs the heats of solution given by the Miedema semiempirical model.[21] For Cd at infinite dilution in Au, this method predicts[12] an alloy shift of 0.11 eV to lower binding energy from the pure Cd metal binding energy. The observed Cd 4*d* core-level position above 60 Å, at which coverages the Cd signal should be completely dominated by the dissociated component, gives a binding energy of -10.75 ± 0.05 eV below E_F for the dissociated Cd $4d_{5/2}$. This binding energy is thus about 0.1 eV higher than the pure metallic binding energy, and 0.2 eV higher than the predicted energy for Cd alloyed in Au. The smallness of these differences, combined with the uncertainty in the alloy shift calculation, does not permit either possibility to be completely ruled out. However, it should be noted that the third possibility noted above, i.e., the presence of the more electronegative Te in the local environment of the dissociated Cd, would be expected to shift the Cd binding energy toward higher binding energy, fully consistent with what is observed. A similar behavior has been seen for dissociated Cd in the Cu/$Hg_{1-x}Cd_xTe$ interface.[9]

D. Schottky-barrier formation

Having shown that in fact the band bending is finished by $\Theta\approx1$ ML, we deduce a final Fermi-level position of $E_F-E_{VBM}=0.8\pm0.1$ eV, implying a Schottky-barrier height of $\sim$0.8 eV to the *p* type sample. A comparison with other experimental results is given in Sec. VI B.

IV. RESULTS: Ag/*n*-TYPE CdTe

A. Overlayer adsorption

He I spectra of the valence-band region with increasing coverage of Ag on the semiconductor substrate are shown in Fig. 6. In the region near E_F, shown on an expanded scale in the inset of the figure, there is emission extending to E_F by the initial coverage of 0.1 ML, while a metallic Fermi edge is detectable by $\Theta=1-2$ ML. As in the case of Au overlayers discussed above, the presence of a Fermi edge at such low overlayer coverages strongly suggests that the overlayer metal is forming clusters on the surface rather than covering the surface

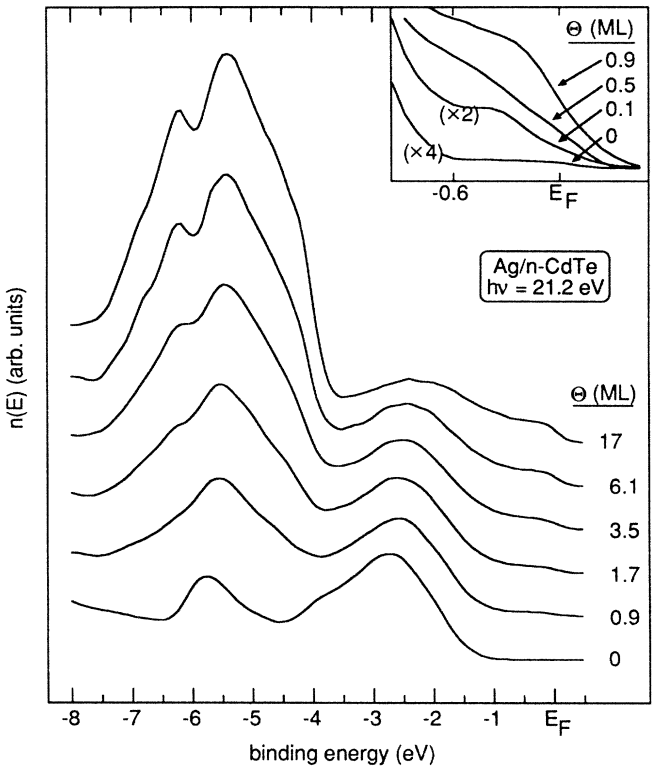

FIG. 6. He I ($h\nu=21.2$ eV) spectra of the valence band with increasing coverage of Ag on CdTe.

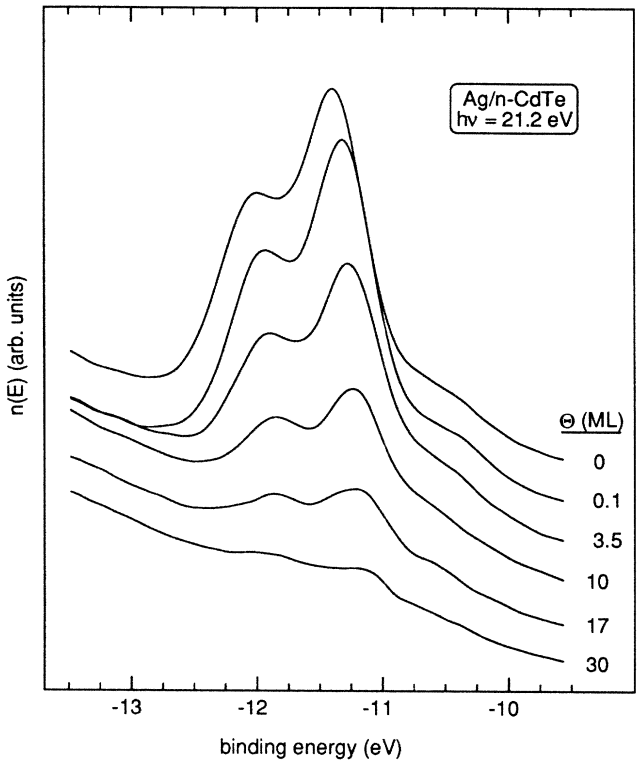

FIG. 7. He I ($h\nu=21.2$ eV) spectra of the Cd 4*d* shallow core levels with increasing coverage of Ag on CdTe. Energies are referred to E_F.

laminarly.

With increasing coverage, Ag 4*d* states centered at about 5.5 eV below E_F arise in the valence-band spectrum; the shape of the Ag 4*d* line has essentially stabilized by 4-ML coverage, with further depositions resulting in an increased Ag 4*d* intensity but little further change in spectral shape. A similar evolution takes place for the Ag 3*d* core level: Between $\Theta=0.1$ and 4 ML the Ag 3*d* peak position shifts 0.2–0.3 eV to higher kinetic energy, stabilizing above the 4-ML coverage at a binding energy of -368.3 ± 0.1 eV for the Ag $3d_{5/2}$ component. As with Au/CdTe, the shift of the overlayer metal core level to lower binding energy with increasing (low) coverage may represent cluster-size effects due to increasing cluster size at higher coverages, or changes in the degree of chemical interaction with the semiconductor substrate.

B. Semiconductor dissociation

The evolution of the Cd 4*d* core levels with Ag deposition is shown in the He I spectra of Fig. 7. In contrast to the cases of Au/CdTe and Cu/CdTe (see Sec. V), for Ag/CdTe there is clearly no dissociated Cd component visible in the spectra, consistent with the observations of Patterson and Williams.[5] Thus the Cd spectra in Fig. 7 originate from the semiconductor substrate, and can therefore be used to extract the band-bending behavior as discussed below in Sec. IV C. Furthermore, the identification of the Cd 4*d* spectra as originating from the substrate, combined with the relatively slow attenuation of these spectral intensities with increasing overlayer coverage, provides information on the growth morphology of the overlayer. The slowness of the Cd attenuation rate is shown more clearly in Fig. 8, which shows the semiconductor core-level intensities I normalized to their zero-coverage values I_0. The Cd 4*d*'s at $h\nu=40.8$ eV attenuate by 35-Å coverage to $I/I_0\approx5\%$, corresponding to an equivalent exponential escape length of about 12 Å, roughly double what one would expect for He II spectra of the Cd 4*d*'s (kinetic energy of ~25 eV). Because this slow attenuation cannot be attributed to Cd dissociation and intermixing with the overlayer, it

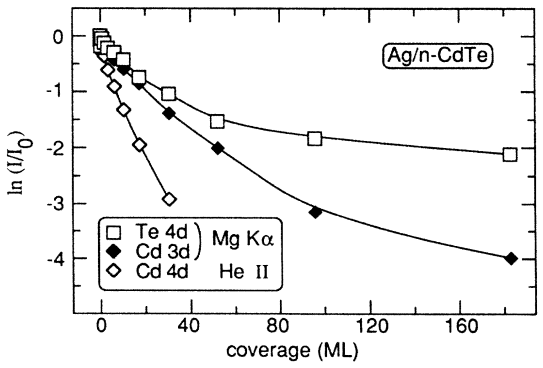

FIG. 8. Attenuation (natural log scale) of the XPS peak areas I of the CdTe core levels with increasing Ag coverage. The peak areas are normalized to their zero-coverage values I_0.

implies that the overlayer distribution on the semiconductor surface is clustered rather than laminar even at coverages as high as 35 Å. Significant clustering of Ag on a CdTe(100) surface prepared by sputter-anneal cycles has been observed by John *et al.*[22]

The attenuation of the Te intensity (also shown in Fig. 8) slows greatly above $\Theta = 35$ Å and almost levels off by $\Theta = 200$ Å. If this lack of attenuation were due solely to clustering of the overlayer, the Cd and Te intensities would attenuate at roughly the same rate.[23] However, as shown in Fig. 8, such behavior is not observed; instead, by $\Theta = 200$ Å the relative attenuation for the Cd $3d$ core intensity is about ten times greater than for the Te $3d$. Therefore, the attenuation of the Te intensity cannot be attributed entirely to clustering of the overlayer and must be due in large part to Te dissociating from the semiconductor and intermixing with the overlayer. The dissociation of Te from the CdTe surface implies the production of dissociated Cd as well. Since no dissociated Cd is observed directly in the photoemission spectra, the dissociated Cd must be localized near the interface under the Ag overlayer, providing a negligible contribution to the spectra, in contrast to the dissociated Te which diffuses out to the overlayer near surface.

By 100-Å coverage the Te $4d_{5/2}$ binding energy has decreased to -39.9 eV relative to the Fermi level. In elemental Te, $E(\text{Te } 4d_{5/2}) - E_{\text{VBM}} = -40.5$ eV,[24] which, assuming E_F does not acquire a degenerate position below the Te VBM, implies $E(\text{Te } 4d_{5/2}) - E_F \geq -40.5$ eV for elemental Te. Since the observed Te binding energy is 0.6 eV lower than this, the dissociated Te at the Ag/CdTe interface must be in reacted form. Elementary (if perhaps naive) charge transfer considerations would predict a shift from the elemental Te binding energy to lower binding energy for Te bound to a cation such as Ag; the observed shift is indeed in this direction.

Examination of the binding-energy region within 4 eV of E_F shows a feature, peaked at -2.5 eV for coverages below 6 ML, which shifts 0.5 eV to higher kinetic energy and decreases in intensity and sharpness with increasing Ag coverage. This feature, which is still visible beyond 60-Å coverage, does not correspond to any spectral feature of Ag metal and instead arises from Te-derived p-like valence states. At high coverages, where the substrate is no longer visible to UPS, this feature originates from dissociated Te in the overlayer.

In contrast to our results, the John *et al.* study[22] shows no evidence for Te dissociation from the semiconductor, but does find Cd floating on the Ag overlayer islands. However, the different surface orientation, CdTe(100), and surface preparation, sputter-anneal cycling, result in an initial semiconductor surface sufficiently different from ours that the different interface morphology is easily understood. Their zero-coverage surface is Cd terminated, and covered with an additional $\frac{1}{4}$ ML of excess Cd; the combination of these two factors seems likely to suppress the Te dissociation that we observe for the stoichiometric CdTe(110) surface. These differences serve to emphasize the importance of surface orientation and preparation upon the morphology of subsequently prepared interfaces.

C. Schottky-barrier formation

Using the value of $E(\text{Cd } 4d_{5/2}) - E_{\text{VBM}} = -10.3$ eV in CdTe,[17] the cleaved-surface Fermi level is located 1.1 ± 0.1 eV above the valence-band maximum; i.e., it is pinned 0.4 eV below the conduction-band minimum for the n-type sample. Upon Ag deposition, E_F shifts down towards the VBM by 0.1–0.15 eV, as reflected in the corresponding shift to higher kinetic energy of the Cd $4d$ states in Fig. 7. The final position of E_F is thus 0.95 ± 0.1 eV above the VBM, implying a Schottky-barrier height of about 0.55 eV to the n-type sample. A comparison with other experimental results is given in Sec. VI B.

V. RESULTS: Cu/CdTe

We summarize here the morphology and band bending of the Cu/n-type CdTe interface, which was discussed in detail in Ref. 9. We also give results for band bending at the Cu/p-type CdTe interface.

A. Morphology

Upon Cu deposition, a well-resolved shifted Cd $4d$ peak originating from dissociated Cd appears in addition to the peak due to metallic Cd; the dissociated Cd peak is the dominant one by 20-Å coverage. Consideration of the attenuation rate of the dissociated Cd signal shows that the dissociated Cd is distributed throughout the overlayer, rather than being segregated at the semiconductor surface. Starting at about 10–15-Å coverage, a significant degree of Te dissociation occurs. The dissociated Te is concentrated largely in a 2–8-Å-thick reacted Cu-Te layer within a few Å of the surface of the overlayer; formation of this Te-rich layer is largely complete by $\Theta = 80$ Å.

B. Schottky-barrier formation

The cleaved-surface Fermi-level position in the Cu/n-type CdTe study was found to lie 1.2 ± 0.1 eV above the VBM, i.e., pinned 0.3 eV below the conduction-band maximum (CBM). Upon Cu deposition, E_F shifted down towards the VBM by ~ 0.2 eV. This shift, complete by the initial deposition of 0.1 ML, puts the final position of E_F at 1 eV above the VBM, i.e., 0.5 eV below the CBM, giving a Schottky-barrier height of ~ 0.5 eV to the n-type sample. For Cu/p-type CdTe, Cu deposition shifted the surface Fermi level up from its cleaved-surface pinning position 0.5 ± 0.1 eV above the VBM to a final position 0.9 ± 0.1 eV above the VBM, giving a Schottky-barrier height of ~ 0.9 eV to the p-type sample. A comparison with other experimental results is given in Sec. VI B.

VI. DISCUSSION

A. CdTe interface morphology

The most striking behavior common to the three noble-metal–CdTe interfaces is the significant motion of dissociated Te from the semiconductor into the over-

layer, so that Te is easily detectable in the overlayer near-surface region at coverages well above 100 Å. For Cu and Au overlayers, this dissociated Te is segregated in a Te-rich layer near the surface of the overlayer. A similar analysis could not be performed for the Ag/CdTe interface as the Te 3*d*/Te 4*d* core-level intensity ratio was not monitored in this case; however, the similarity in the attenuation behavior of the Te 4*d* for Ag overlayers with the attenuation for Au and Cu overlayers suggests that the dissociated Te in the Ag overlayer may well be concentrated near the surface as it is for the other two noble-metal overlayers.

For Ag and Cu, and possibly Au, the dissociated Te from the semiconductor is in reacted form with the overlayer metal. The dissociation of Te from the CdTe substrate and subsequent reaction with the overlayer metal, appears inconsistent with the bulk thermodynamic data of Table I, which shows the CdTe bond strength to be much greater than any of the noble-metal–CdTe compounds. As always, surface and interface effects must be considered along with the bulk thermodynamics. For instance, the heat of condensation of the overlayer metal on the semiconductor could well provide some of the energy needed for dissociation of Te from the CdTe substrate. Once the dissociation has been accomplished, the next step of reaction with the overlayer is favored by bulk thermodynamics.

For Au and Cu overlayers, but not for Ag overlayers, there is dissociated Cd in the overlayer near surface. Examination of the $\Delta H_{\rm sol}(\mathrm{Cd};M)$ values from Table I shows that Cd has a high negative enthalpy of solution in Au, which would tend to favor dissociated Cd being pulled into the overlayer. However, while both Cu and Ag have similar small enthalpies of solution for Cd, only for the former overlayer metal is a significant quantity of dissociated Cd pulled into the overlayer near-surface, again pointing up a limitation in the use of simple bulk thermodynamic data in attempting to predict complex interface behavior.

B. Schottky-barrier formation

A tabulation of noble-metal–CdTe Schottky-barrier heights for vacuum-fabricated interfaces from other experiments[3–5,22,25–30] as well as ours is given in Table II, presented in the form of $E_F - E_{\rm VBM}$. For each of the three overlayer metals, the majority of the measurements, which included the use of electrical and photoresponse techniques as well as photoemission, lie within ~ 0.1 eV of ours. This agreement supports the interpretation of the present results as representing the "true" Schottky-barrier heights within ± 0.1 eV. This will be assumed in the following discussion.

TABLE I. Heats of telluride formation ΔH_f, and heats of solution $\Delta H_{\rm sol}(\mathrm{Cd};M)$ of Cd at infinite dilution in metal M, for the noble metals on CdTe.

Metal (M)	Telluride	ΔH_f[a] (kcal/mol)	$\Delta H_{\rm sol}(\mathrm{Cd};M)$[b] (kcal/mol)
Cd	CdTe	−24.1	
Ag	Ag_2Te	−8.6	−3.4
Cu	Cu_2Te	−10.0	−1.7
Au	$AuTe_2$	−4.5	−12.2

[a]From Ref. 2.
[b]Calculated from Miedema's semiempirical model (Ref. 21).

The Fermi-level pinning positions for the three noble metals all fall within a narrow range of about 0.2 eV. Because the work functions ϕ_m of the noble metals span a range of 0.8 eV, with $\phi_m(\mathrm{Au}) = 5.1$ eV and $\phi_m(\mathrm{Ag}) = 4.3$ eV,[31] the suggested strong dependence[3–5,28] of Schottky-barrier height on metal work function for metal-CdTe interfaces is not supported by the present data.

The narrow range of Fermi-level pinning is more consistent with defect[32] or Tersoff-type[33,34] (MIGS) models of Schottky-barrier formation. Williams *et al.*[3–5] and Brucker and Brillson[35] have suggested that defects such as Cd vacancies may play a role in determining the Schottky-barrier height, although a calculation by Kobayashi *et al.*[36] gives a cation vacancy energy level below the VBM in CdTe. The $\mathrm{Te_{Cd}}$ antisite, calculated[36] to lie about 1 eV above the VBM, would be a more likely candidate for Fermi-level pinning in the context of a defect model. For the Tersoff model, Tersoff's "midgap" energy lies 0.85 eV above the VBM for CdTe,[34] consistent with the Fermi-level pinning observed in the present work.

C. Comparison with $Hg_{1-x}Cd_xTe$

Te dissociation and intermixing with the overlayer, discussed above for the CdTe interfaces, is very frequently observed in metal-$Hg_{1-x}Cd_xTe$ interfaces as well.[7–12] The extent of the Te dissociation is generally much more pronounced for $Hg_{1-x}Cd_xTe$ (MCT) than for CdTe. For instance, for Cu/MCT the Te concentration in the overlayer near-surface at high coverages is about 35%, an order of magnitude more than for Cu/CdTe.[9] The enhanced Te dissociation for MCT can be understood in terms of disruption of the MCT surface lattice due to depletion of the weakly bound Hg from the surface.

Of the three noble metals on CdTe, Ag stands out as the one for which no Cd is observed in the overlayer near-surface region. It is interesting to note that Ag also differs from the other two noble metals in its behavior on MCT. Cu/MCT (Ref. 9) and Au/MCT (Ref. 10) have similar interface morphologies, with at most a limited indiffusion of the overlayer metal into the semiconductor. In comparison, for Ag/MCT there is a massive motion of the overlayer metal into the semiconductor as Ag atoms replace Hg atoms in the lattice.[8] Further investigation into the causes of Cd dissociation from CdTe may conceivably also provide insight into the question of overlayer indiffusion for MCT.

VII. SUMMARY

None of the three noble-metal–CdTe interfaces is entirely abrupt: all three show Te dissociation into the overlayer. For Ag and Cu, and possibly Au, the dissociated Te is in reacted form with the overlayer metal. For

TABLE II. Fermi-level pinning positions relative to the VBM for noble metals on CdTe, from this work and other references. The corresponding Schottky-barrier heights ϕ_{Bn} and ϕ_{Bp} to n- and p-type material are $\phi_{Bp}=E_F-E_{\rm VBM}$, $\phi_{Bn}=E_g-\phi_{Bp}$.

Overlayer metal	Semiconductor conductivity	$E_F-E_{\rm VBM}$ (eV)	Method[a]	Reference
Cu	n	1.0	PE	this work
	n	1.3[b]	PE	3
	n	1.05[c]	I-V	5
	n	1.01[c]	I-V, PR	25
	p	0.9	PE	this work
Ag	n	0.95	PE	this work
	n	0.96	PE	22
	n	1.0(1.5)[b]	PE	4
	n	>1.2[c]	C-V	4
	n	0.69[c,d]	C-V	26
	n	0.84[c]	PR	26
Au	n	0.65[b]	PE	4
	n	0.79[c,d]	C-V	26
	n	0.54[c]	C-V	4
	n	0.81[c]	C-V	25
	n	0.90[c]	I-V	26
	n	0.85[c]	I-V, C-V, PR	27
	n	0.90[c]	I-V, PR	25
	p	0.8	PE	this work
	p	0.65	I-V, C-V	28

[a]PE: Photoemission; I-V: I-V electrical; C-V: C-V electrical; PR: photoresponse.
[b]See comments in Ref. 30.
[c]Calculated from $E_F-E_{\rm VBM}=E_g-\phi_{Bn}$, with $E_g=1.50$ eV.
[d]Quoted by Sze (Ref. 29).

Cu and Au overlayers, and possibly also for Ag overlayers, the dissociated Te from the semiconductor is concentrated largely in a region within 10–20 Å of the surface of the overlayer. Dissociated Cd is observed for Cu and Au overlayers, but not for Ag overlayers. While all three overlayers may be distributed on the CdTe surface as islands for coverages below a few monolayers, for Ag overlayers clustering is observed for coverages as high as 35 Å, and possibly much higher. The Fermi level after metal deposition fell 0.8–1.0 eV above the VBM for all the interfaces studied.

ACKNOWLEDGMENTS

This work was supported by the U. S. Defense Advanced Research Projects Agency Contract No. MDA-903-83-C-0108. Some of the crystals used in the Stanford University experiments were grown at Santa Barbara Research Center.

[1]L. J. Brillson, Surf. Sci. Rept. **2**, 123 (1982).
[2]K. C. Mills, *Thermodynamic Data for Inorganic Sulphides, Selenides and Tellurides* (Butterworths, London, 1974).
[3]R. H. Williams and M. H. Patterson, Appl. Phys. Lett. **40**, 484 (1982).
[4]T. P. Humphreys, M. H. Patterson, and R. H. Williams, J. Vac. Sci. Technol. **17**, 886 (1980).
[5]M. H. Patterson and R. H. Williams, J. Cryst. Growth **59**, 281 (1982).
[6]R. R. Daniels, G. Margaritondo, G. D. Davis, and N. E. Byer, Appl. Phys. Lett. **42**, 50 (1983).
[7]G. D. Davis, N. E. Byer, R. A. Riedel, and G. Margaritondo, J. Appl. Phys. **57**, 1915 (1985).
[8]D. J. Friedman, G. P. Carey, C. K. Shih, I. Lindau, W. E. Spicer, and J. A. Wilson, J. Vac. Sci. Technol. A **4**, 1977 (1986).
[9]D. J. Friedman, G. P. Carey, I. Lindau, and W. E. Spicer, Phys. Rev. B **34**, 5329 (1986).
[10]G. D. Davis, W. A. Beck, N. E. Byer, R. R. Daniels, and G. Margaritondo, J. Vac. Sci. Technol. A **2**, 546 (1984).
[11]A. Franciosi, P. Phillip, and D. J. Peterman, Phys. Rev. B **32**, 8100 (1985).
[12]D. J. Friedman, G. P. Carey, I. Lindau, and W. E. Spicer, Phys. Rev. B **35**, 1188 (1987).
[13]J. Chu, S. Xu, and D. Tang, Appl. Phys. Lett. **43**, 1064 (1983).

[14]W. E. Spicer, J. A. Silberman, I. Lindau, A.-B. Chen, A. Sher, and J. A. Wilson, J. Vac. Sci. Technol. A **1**, 1735 (1983).

[15]M. G. Mason, Phys. Rev. B **27**, 748 (1983).

[16]I. Lindau and W. E. Spicer, in *Synchrotron Radiation Research,* edited by H. Winick and S. Doniach (Plenum, New York, 1980).

[17]J. A. Silberman, Ph. D. thesis, Stanford University, 1986, p. 51. The VBM in these studies was located with angle-resolved photoemission at normal emission. For CdTe at photon energies near 21 eV, normal emission is much more heavily weighted by states near the VBM than is the off-normal emission detected by the CMA, permitting a more accurate determination of the VBM.

[18]J. Nogami, T. Kendelewicz, I. Lindau, and W. E. Spicer, Phys. Rev. B **34**, 669 (1986).

[19]*Photoemission in Solids I,* edited by M. Cardona and L. Ley (Springer-Verlag, Berlin, 1978).

[20]P. Steiner and S. Hüfner, Acta Metall. **29**, 1885 (1981).

[21]A. R. Miedema, P. F. de Châtel, and F. R. de Boer, Physica **100B**, 1 (1980).

[22]P. John, T. Miller, T. C. Hsieh, A. P. Shapiro, A. L. Wachs, and T.-C. Chiang, Phys. Rev. B **34**, 6704 (1986).

[23]The dependence of photoelectron escape length on electron kinetic energy (Ref. 16) shows that the escape lengths λ(Te $3d$) and λ(Cd $3d$) excited by Mg $K\alpha$ light are nearly equal: $\lambda(\text{Cd } 3d)/\lambda(\text{Te } 3d) < 1.3$. This difference would not be nearly enough to explain the difference between the Cd $3d$ and Te $3d$ attenuations. In fact, if one assumed only clustering and no dissociation, at high coverages the Cd and Te signals would be dominated by the remaining uncovered regions of the CdTe, and the Cd and Te signals would attenuate to an equal degree.

[24]N. J. Shevchik, M. Cardona, and J. Tejeda, Phys. Rev. B **8**, 2833 (1973).

[25]T. Takebe, J. Seraie, and T. Tanaka, Phys. Status Solidi A **47**, 123 (1978).

[26]C. A Mead and W. G. Spitzer, Phys. Rev. **134**, A713 (1964).

[27]T. F. Kuech, J. Appl. Phys. **52**, 4874 (1981).

[28]J. G. Werthen, J.-P. Häring, A. L. Fahrenbruch, and R. H. Bube, J. Appl. Phys. **54**, 5982 (1983).

[29]S. M. Sze, *Physics of Semiconductor Devices* (Wiley, New York, 1981).

[30]Williams *et al.* (Refs. 3–5) assume the Schottky barrier height ϕ_B to be the *shift* $\Delta E_{F,s}$ in the surface Fermi level $E_{F,s}$ upon overlayer deposition. Only if the cleaved surface Fermi level $E_{F,i}$ is at the conduction-band minimum (for n-type samples) will this shift be equal to $\phi_{Bn} = E_{F,s}(\text{final}) - E_{\text{CBM}}$. However, $E_{F,i}$ is often located below the CBM, as for example in the present work. The exact location of $E_{F,s}$ is widely believed to depend on the quality of the cleave. Even the bulk Fermi level may lie below the CBM depending on the sample doping. Thus it is dangerous to deduce Schottky-barrier heights from $E_{F,s}$ shifts alone. For example, for Ag/n-type CdTe Williams *et al.* (Refs. 3–5) observe no $E_{F,s}$ shift and so quote $\phi_{Bn} = 0$. However, a direct examination of their photoelectron spectra (Ref. 4) shows $E_{F,s}(\text{final}) - E_{\text{VBM}} \approx 1$ eV, roughly in agreement with our results. For Au/CdTe the Cd dissociation prohibits the extraction (as in Sec. III C) of $E_{F,s}(\text{final}) - E_{\text{VBM}}$ from their spectra (Ref. 4), while they appear not to have published spectra for Cu/CdTe.

[31]H. B. Michaelson, J. Appl. Phys. **48**, 4729 (1977).

[32]W. E. Spicer, I. Lindau, P. Skeath, C. Y. Su, and P. Chye, Phys. Rev. Lett. **44**, 420 (1980).

[33]J. Tersoff, Phys. Rev. B **32**, 6968 (1985).

[34]J. Tersoff, Phys. Rev. Lett. **56**, 2755 (1986).

[35]C. F. Brucker and L. J. Brillson, Thin Solid Films **93**, 67 (1982).

[36]A. Kobayashi, O. F. Sankey, and J. D. Dow, Phys. Rev. B **25**, 6367 (1982).